Modeling the inhibition of quadruple mutant *Plasmodium falciparum* dihydrofolate reductase by pyrimethamine derivatives

Gary B. Fogel · Mars Cheung · Eric Pittman · David Hecht

Abstract Modeling studies were performed on known inhibitors of the quadruple mutant *Plasmodium falciparum* dihydrofolate reductase (DHFR). GOLD was used to dock 32 pyrimethamine derivatives into the active site of DHFR obtained from the x-ray crystal structure 1J3K.pdb. Several scoring functions were evaluated and the Molegro Protein-Ligand Interaction Score was determined to have one of the best correlation to experimental pK_i. In conjunction with Protein-Ligand Interaction scores, predicted binding modes and key protein-ligand interactions were evaluated and analyzed in order to develop criteria for selecting compounds having a greater chance of activity versus resistant strains of *Plasmodium falciparum*. This methodology will be used in future studies for selection of compounds for focused screening libraries.

Keywords Dihydrofolate reductase · Malaria · Molecular docking · Evolutionary computation

Introduction

According to the CDC, approximately forty-one percent of the world's population live in areas where malaria is transmitted (e.g., parts of Africa, Asia, the Middle East, Central and South America, Hispaniola, and Oceania) [1]. Each year it is estimated that between 350–500 million cases of malaria occur worldwide, and over one million people die, most of them young children in sub-Saharan Africa [1]. Although malaria is thought to have been eradicated from North America and Europe (through the widespread application of pesticides such as DDT), some scientists predict a re-emergence of the disease [2].

In addition to pesticides, the use of bed nets and of anti-malarial pharmaceuticals has been shown to dramatically reduce mortality rates [1]. Unfortunately most of the population at risk lives in poverty and cannot afford these life-saving technologies. The average cost for an insect treated net is $5.00 [3] and the average costs of some of the most common malaria drugs are estimated to be: $0.13 per dose for chloroquine, $0.14 per dose for sulfadoxine-pyrimethamine, and $2.68 for a 7-day course of quinine [1].

This problem is compounded by the fact that two of the most prevalent strains, *Plasmodium falciparum* (*Pf*) and *Plasmodium vivax* (*Pv*) have developed clinical resistance to antifolate compounds such as pyrimethamine and cycloguanil. Once thought to be long-term solutions to malaria infection, these compounds target dihydrofolate reductase (DHFR)-thymidylate synthase, a well-known and validated target for anti-malarial drugs [4–6]. DHFR catalyzes several key steps in the synthesis of purines, pyrimidines, and some amino acids. Inhibition of DHFR effectively blocks DNA synthesis and leads to death of prokaryotes and unicellular eukaryotes such as *Pf* and *Pv* [7]. In addition to malaria, DHFR has been a validated target for cancer [8] as well as for a wide range of bacterial infections [9]. This resistance arises from amino acid substitutions [10–12] in *Pf*-DHFR at residues 51, 59, 108 and 164 and *Pv*-DHFR at residues 58, 117, and 173.

Recent efforts to identify new small molecule anti-malarial drugs have focused on applications of structure-based

G. B. Fogel · M. Cheung
Natural Selection, Inc., 9330 Scranton Road,
Suite 150,
San Diego, CA 92121, USA

E. Pittman · D. Hecht (✉)
Southwestern College, 900 Otay Lakes Road,
Chula Vista, CA 91910, USA
e-mail: dhecht@swccd.edu

design and discovery [13–14]. These include: x-ray crystal-lography [10, 12], molecular modeling [15], and quantitative structure-activity relationships (QSAR) [16–24]. These efforts have resulted in the successful discovery of a third generation antifolate active compound, WR99210, against resistant strains of both *Pf* and *Pv* [25] WR99210 was discovered over twenty years ago and has been the basis for multiple structure-activity relationship (SAR) studies. From these studies a bridge of 3 carbons linking two aromatic ring systems has been identified as being important for activity. As will be shown below, this allows these compounds to avoid steric clashes in the quadruple mutant-binding site.

One promising approach for improving the efficiency and productivity of early discovery is through the use of "focused" compound screening libraries [26]. Protein-ligand docking algorithms are commonly used in virtual high-throughput screening (vHTS) to filter through large libraries of compound structures. Compounds are ranked and selected for focused screening libraries based on their predicted relative binding affinities. In addition, this approach provides models of the predicted binding mode(s) and conformation(s) in an active site. These models can be useful in selection of compounds as well as in the generation and evaluation of SAR hypotheses. In a recent review [26], protein-ligand docking algorithms were organized into the following categories: Fast Shape Matching (DOCK and Eudock); Incremental Construction (FlexX, Hammerhead, SLIDE); Tabu search (PRO_LEADS, SFDock); Evolutionary Algorithms (GOLD, AUTODOCK, Gambler); Monte Carlo (MCDock, QXP); and Distance Geometry (Dockit).

While docking algorithms often successfully predict the bound conformations of a ligand (often down to <1 Å rmsd of the experimentally determined bound conformation) they have a more difficult time predicting binding affinities correctly [27–30]. In addition, most algorithms do not allow for side-chain or back-bone movement in the binding pocket, ignoring conformational changes that occur upon binding [31, 32]. Depending upon the target of interest, these deficiencies have varying significance.

In this study, we performed docking studies with GOLD using known inhibitors of the quadruple mutant *Pf*-DHFR inhibitors in order to develop models that not only provide details of the binding mode and key molecular interactions, but also allow for prediction of relative inhibition and binding affinities.

Materials and methods

Docking protocols

In order to develop the docking methodology, we first attempted to demonstrate that bound conformations

could be reproduced *in silico*. For this purpose, the x-ray crystal structures of both *Plasmodium falciparum* wild-type DHFR-TS (1J3I.pdb) [10] and quadruple mutant DHFR-TS (1J3K.pdb) [10] were selected. Both of these structures contain the third-generation *Pf*-DHFR inhibitor WR99210 bound to the active site in the presence of NADPH, and are assumed to be representative of bound conformations in vivo.

The first step in preparation of the receptor was to remove all waters as well as other non-protein, non-ligand or non-cofactor molecules. For this purpose, Deepview (Swiss-PDBviewer) [33] was used. In order to simplify the docking calculations, the DHFR crystal structures were truncated to a 10 Å radius from each atom in the bound WR99210 inhibitor.

The protein-ligand interactions of the bound conformations of WR99210 were examined in order to identify a suitable binding site center atom for purposes of defining the binding site in the docking software, GOLD. The carbonyl oxygen on Leu 164 (for 1J3K.pdb) and Ile 164 (for WT 1J3I.pdb) were selected. These atoms are located deep in the pocket close to the center of the bound WR99210.

The inhibitor WR99210 was then removed, the NADPH cofactor was retained, and the resulting *.pdb files were imported into MOE [34]. The "wash" function in MOE was used to add explicit hydrogen atoms and to set atom ionization states based on their formal charges. Finally, the protein structures were exported as *.pdb files for input into GOLD [35].

The WR99210 structure was drawn using Chemdraw (Cambridgesoft, Inc.) [36] and exported to MOE as a *.mol file. Hydrogen atoms were added to the two-dimensional structure and atom ionization set to formal charge using the "wash" function in MOE before conversion to three-dimensions and minimization using the MMFF94x37 gas phase potential. The structure was then exported in *.sdf format for input to GOLD.

Docking experiments were performed using the default GOLD fitness function (VDW = 4.0, H-bonding = 2.5) and evolutionary parameters: population size = 100; selection pressure = 1.1; # operations = 100,000; # islands = 5; niche size = 2; migration = 10; mutation = 95; crossover = 95 [35]. The carbonyl oxygen on Leu 164 (for 1J3K.pdb) and Ile 164 (for WT 1J3I.pdb) was selected as the binding site center for all calculations.
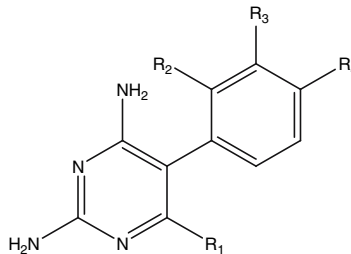
Ten docking runs were performed per structure. If at any time 3 of the 10 poses were within 1.5 Å rmsd of each other, the docking run for that structure was terminated and docking calculations began for the next structure. All poses and docking scores were outputted into a single *.sdf file and text file respectively.

Scoring function selection

Thirty-two compounds with experimentally-derived quadruple mutant Pf-DHFR K_i values were obtained from the literature [16, 17]. All compounds (Table 1) were drawn using Chemdraw (Cambridgesoft, Inc.) [36] and then imported into MOE. The 2-dimensional structures were "washed," converted to three dimensions, and minimized using the MMFF94x [37] gas phase potential. The structures were finally exported in *.sdf format for import to GOLD.

Table 1 Structures, experimental pK_i values and docking scores are listed [16, 17]. Compounds with unrealistic poses were considered inactive and are indicated with an asterisk (*) in the Protein-Ligand Score column

ID	R1	R2	R3	R4	pKi_{mutant}	Protein- ligand score (Mut)
P39	$-C_6H_{13}$	H	H	H	8.85	−105.21
P40	$-(CH_2)_2O(CH_2)_3OC_6H_5$	H	Cl	H	8.77	−132.48
P32	$-(CH_2)_3C_6H_4-(p-OCH_3)$	H	Cl	H	8.70	−116.14
P31	$-(CH_2)_3C_6H_5$	H	Cl	H	8.70	−116.66
P29	$-(CH_2)_3COOCH_3$	H	Cl	H	8.57	−106.63
P30	$-CH_2CH_3$	H	Cl	H	8.48	−88.95
P43	$-(CH_2)_3OCOC_6H_5$	H	Cl	H	8.44	−122.15
P44	$-(CH_2)_3OCOOCH_2C_6H_5$	H	Cl	H	8.44	−126.37
P33	$-(CH_2)_3C_6H_5$	H	H	H	8.33	−113.89
P47	$-(CH_2)_3OCOC_6H_5$	H	H	H	7.85	−119.05
P38	$-CH_3$	H	Cl	H	7.85	−87.49
P26	$-(CH_2)_3COOCH_3$	H	H	H	7.62	−105.85
P42	$-(CH_2)_3OCOCH_3$	H	Cl	H	7.50	−112.44
P20	$-CH_2CH_3$	H	H	H	7.50	−88.75
P13	$-CH_2CH_3$	H	Cl	Cl	7.27	−85.83
P41	$-(CH_2)_3OH$	H	Cl	H	7.24	−93.71
P12	$-(CH_2)_3C_6H_5$	H	H	Cl	6.77	−99.71
P46	$-(CH_2)_3OCOCH_3$	H	H	H	6.63	−103.89
P15	$-CH_2CH_3$	H	OCH_2O		6.57	−87.31
P17	$-CH_2CH_3$	H	H	CH_3	6.55	−85.35
P21	$-CH_2CH_3$	H	H	Br	6.52	−84.88
P7	$-CH_2CH_2CH_3$	H	H	Cl	6.44	−86.23
P16	$-(CH_2)_3COOCH_3$	H	H	Cl	6.44	−95.57
Pyr	$-CH_2CH_3$	H	H	Cl	6.41	−81.57
P2	$-CH(CH_3)_2$	H	H	Cl	6.27	−84.65
P45	$-CH_2OH$	H	H	H	6.26	−85.62
P18	$-CH_2CH_3$	H	H	OCH_3	6.21	−90.83
P3	$-CH_2CH(CH_3)_2$	H	H	Cl	6.10	−91.40
P5	$-C_6H_4-(p-OCH_3)$	H	H	Cl	5.80	*−84.66
P14	$-CH_2CH_3$	Cl	H	Cl	5.73	−68.04
P4	$-C_6H_5$	H	H	Cl	5.46	*−88.57
1h	$-CH_3$	H	H	H	n/a	*−77.51

Docking experiments were performed using the truncated quadruple mutant active site (1J3K.pdb) as described above. A single desktop computer operating with Win XP Media edition (AMD 3800+, 64 bit processor (~2.65 GHz) and 1 GB RAM) processed 25 compounds in ~3 h.

The output from GOLD was imported into Molegro Virtual Docker (Molegro ApS) [38]. Visual inspection of all poses was then performed to eliminate poses where the diaminopyrimidine ring did not superimpose on the bound WR99210 x-ray conformation with rmsd ≤ 1 Å. In 3 cases, P4, P5 and 1 h all poses were eliminated. A final round of filtering was performed to eliminate all but the top scoring (GOLDscore) pose.

Using these filtered poses, an evaluation of different docking algorithms and scoring functions was performed. These included "Goldscore" and "Chemscore" (GOLD) [35], XScore (Univ. of Michigan) [27], Score (Univ. of Beijing) [28], several scoring functions in Molegro [38], LigScore1, and LigScore2 [39], Piecewise Linear Potential - PLP1 [40], PLP2 [41], Jain [42], and PMF [43] (Accelrys' Discovery Studio).

Results

The goal of this paper was to develop methodology for selecting compounds having a greater chance of activity versus resistant strains of *Plasmodium falciparum*. This methodology will be used in future studies for selection of compounds for focused screening libraries.

Two assumptions were central to this approach: 1) the poses resulting from *in silico* docking represented the correctly bound conformations, and 2) the values generated from a scoring function correlated with experimentally measured binding affinities of ligands for an active site.

Pose evaluation

In order to test the validity of assumption #1, we docked the inhibitor WR99210 into the active site of wild-type *Pf*-DHFR-TS crystal structure (1J3I.pdb) as well as the active site of the quadruple mutant crystal structure (1J3K.pdb). The resulting docked conformations of WR99210 (to both wild-type and quadruple mutant x-ray crystal structures) fell within 1.1 Å rmsd for all atoms from the bound x-ray conformations (Fig. 1).

For 24 of the compounds, the docking runs resulted in poses that were not within 1.5 Å rmsd of each other. This is most likely due to the presence of large and flexible r-groups primarily in position R1 (Table 1). As seen in Figs. 1 and 2, the diaminopyrimidine rings of 29 of the

poses superimpose nicely on each other and on the x-ray conformation of WR99210 (rmsd < 1 Å). This ring as well as the second ring of the template are found to bind deep in the binding site where there is very little room for alternative conformations. The R1 group is solvent accessible and appears to make contacts with surface residues, thus allowing for the possibility of greater conformational variability.

It often occurred, in each set of 10 poses per compound, that the diaminopyrimidine rings did not superimpose on that of the bound conformation of WR99210 within 1 Å rmsd. For most cases these were fairly obvious by visual inspection (Fig. 2) and easily removed in Molegro. In some cases, the diaminopyrimidine rings of the poses both superimposed on that of the bound conformation of WR99210, but fell into one of two cluster classes illustrated in Fig. 3 in which the diaminopyrimidine rings were rotated 180° with respect to each other.

An analysis of the protein-ligand contacts was then performed to further study the differences between the two poses. Figure 4 shows the protein contacts made by the x-ray crystal determined conformation of WR99210, and the two docking poses of 1 h.

Previous studies have identified Asp 54 as a critical active site residue involved in hydrogen bonding to the substrate [5, 10–12]. From analysis of the x-ray structures [10], as well as the poses presented here, it appears that WR99210 can have two possible H-bonding contacts to Asp 54. In addition, there appears to be another potential H-bond with Ile 14. The position and length of the 3-carbon connector has also been documented to be a key feature in WR99210's activity [25] avoiding unfavorable steric clashes with Asn 108.

For both poses of compound 1 h, there appear to be fewer contacts/interactions with the active site residues than for WR99210. Both poses of 1 h have only one H-bonding contact with Asp 54. However, the second pose (Figs. 3b and 4c) lost two potential H-bonding interactions with Ile 14 and Leu 164 (one of the four altered residues) and instead gained a potential H-bonding interaction with the Thr 185 side chain (see Fig. 4c). In lieu of experimental data, this analysis supports the selection of the other pose (Figs. 3a and 4b) as these key H-bonding interactions with Ile 14 and Leu 164 are retained. Similar analyses were performed in order to filter out other poses from the docking results.

Scoring function analysis and selection

One major weakness of protein-ligand docking algorithms is the apparent disconnect of the docking scores from experimental binding affinities [27–30]. Even though

Fig. 1 Superposition of WR99210 conformations obtained from x-ray structure and docking experiments. (**a**) WR99210 from wt *Pf*-DHFR-TS (1J31.pdb) in orange and the docked conformation in CPK, rmsd = 1.095 Å. (**b**) WR99210 from quadruple mutant *Pf*-DHFR-TS (1J3K.pdb) in orange and the docked conformation in CPK rmsd = 0.951 Å. (**c**) Superposition of 28 docked compound poses [16, 17] in CPK on the bound x-ray crystal of WR99210 (1J3K.pdb) in orange, rmsd < 1 Å for the diaminopyrimidine rings
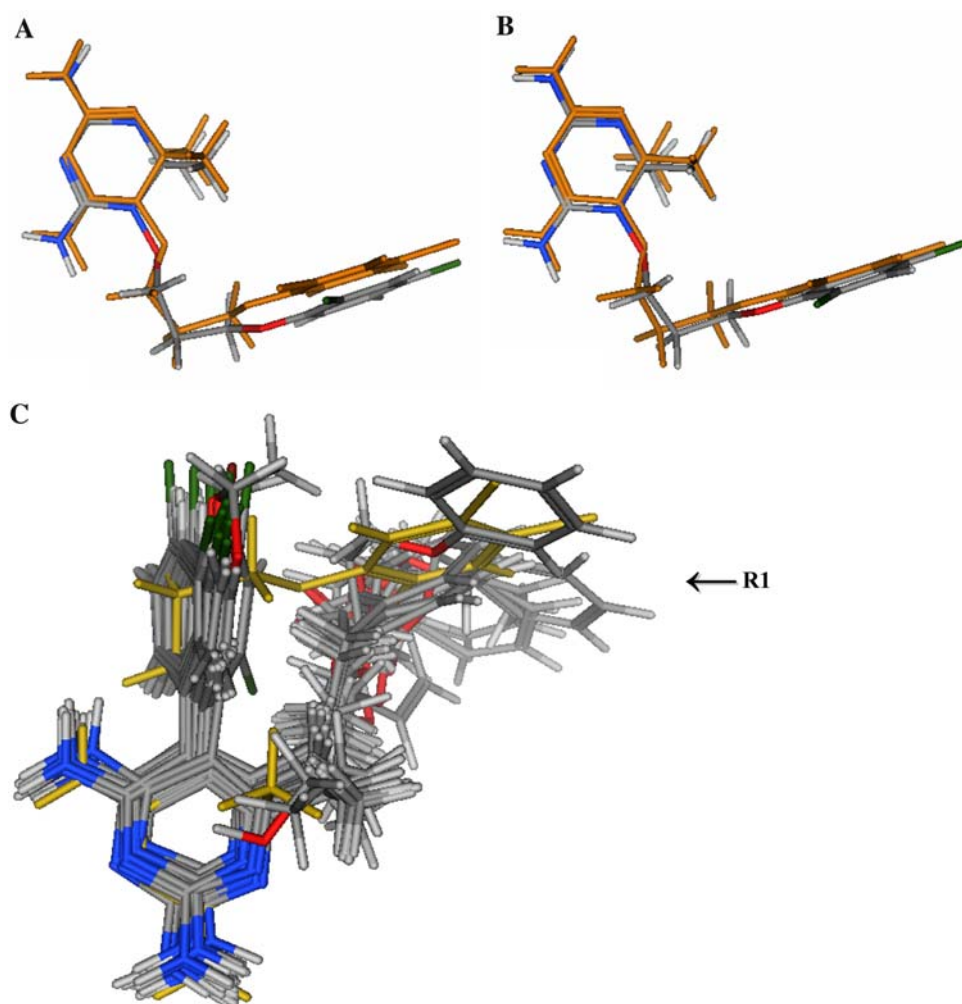
Fig. 2 (**a**) Superposition of a compound pose on the bound x-ray conformation of WR99210 (in orange). (**b**). Superposition of 3 poses, two consistent with that of WR99210 and 1 inconsistent. (**c**). Same as (**b**) with the inconsistent pose removed
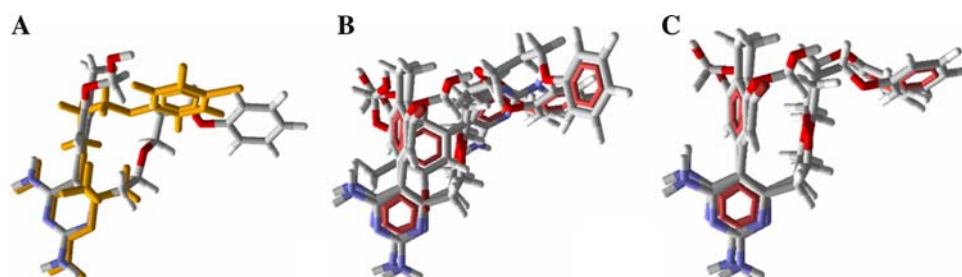

Fig. 3 (**a**). Superposition of one pose of compound 1 h[17] on the bound x-ray conformation of WR99210. B). Superposition of another pose with the diaminopyrimidine ring rotated 180°
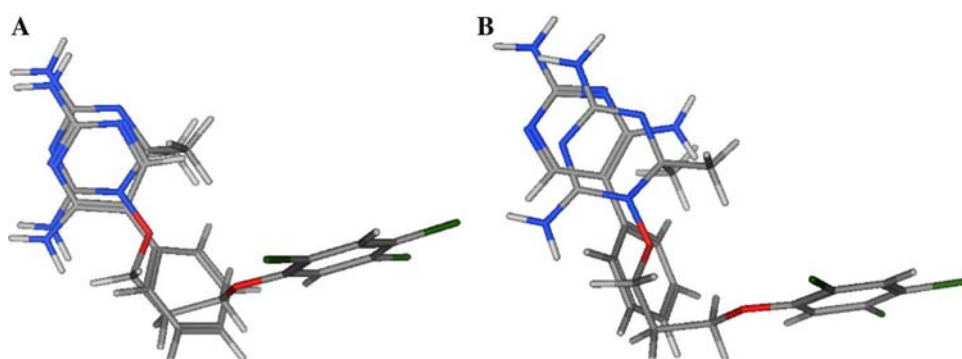
Fig. 4 Key protein-ligand contacts of bound WR99210 to: (**a**). Wild-type *Pf*-DHFR (1J3I.pdb) and (**b**). quadruple mutant *Pf*-DHFR (1J3K.pdb). (**c**). Protein contacts of one pose of 1 h. (**d**). Contacts of another pose of 1 h with its diaminopyrimidine ring are rotated 180°
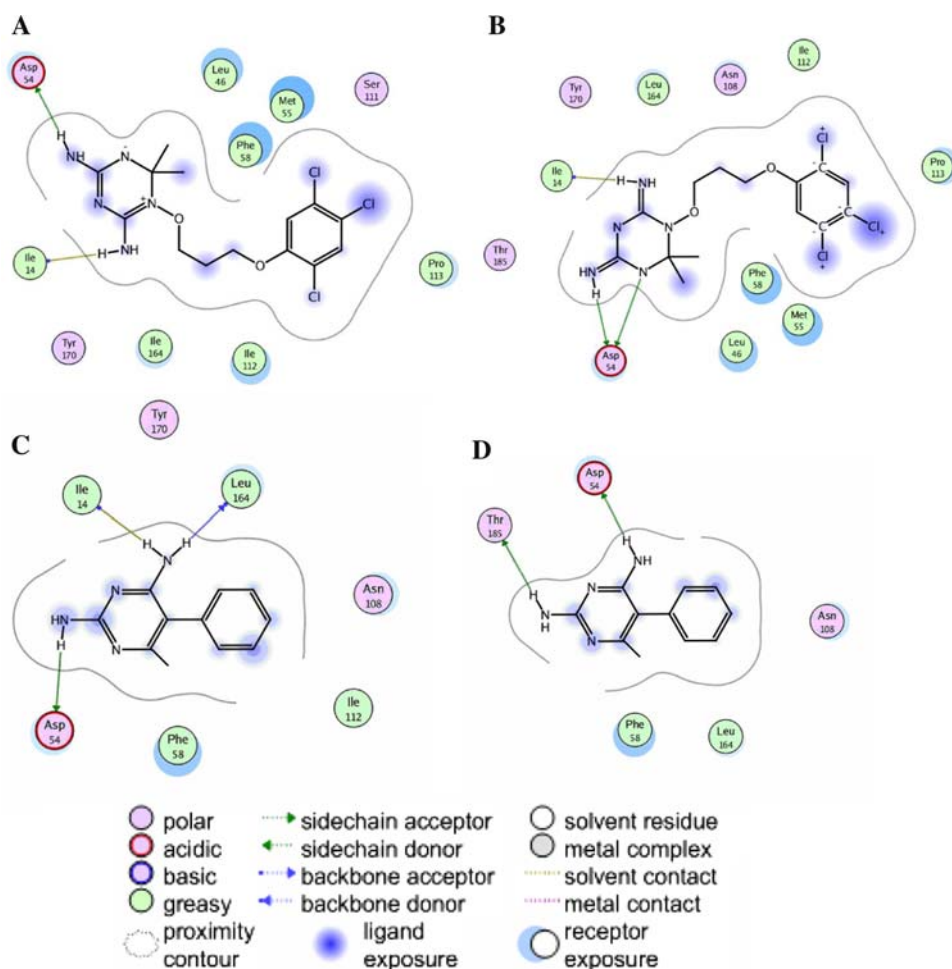
"correct" bound conformations can often be calculated, the predicted binding affinities (and more importantly the relative ranking of binding affinities) for a set of small molecules are often wrong. Determination that the values generated from a scoring function correlate with real, experimentally measured, binding affinities of ligands for an active site, is a test of assumption #2 above.

Using the 32 filtered poses of compounds bound to quadruple mutant *Pf*-DHFR, an evaluation of different docking algorithms and scoring functions was performed. These included "Goldscore" and "Chemscore" (GOLD) [35], XScore (Univ. of Michigan) [27], Score (Univ. of Beijing) [28], several scoring functions in Molegro [38], and LigScore1 and LigScore2 [39], Piecewise Linear Potential—PLP1 [40], PLP2 [41], Jain [42], and PMF [43] (Accelrys' Discovery Studio). The linear correlations with experimental pK_i for each are presented in Table 2. The top linear correlations for the 32 pyrimethamine analogues were found using Accelrys' LigScore1 ($R^2 = 0.69$) and Molegro's "Protein-Ligand Interaction" score ($R^2 = 0.68$).

In general, these scoring functions tend to fall into two major classes emphasizing either: H-bonding interactions or van der Waals, hydrophobic as well as polar attractive/repulsive interactions. GOLDscore, Xscore, PLP (1&2), as well as the Molegro scoring functions all have highly weighted H-bonding terms. On the other hand, LigScore (1&2), Jain, PMF, and Chemscore contain highly weighted terms for van der Waals interactions, lipophilic interactions, and polar attractive/repulsive interactions as well as terms for buried and total polar surface areas. As H-bonding appears to play a critical role in the binding of the 32 pyrimethamine analogues presented, it is not surprising that the scoring functions with H-bonding terms seemed to do better (in terms of correlation with pK_i values). XScore and LigScore1 were exceptions (Table 2).

As described previously, all poses were generated using GOLD with a static binding site. The scoring of the poses therefore does not take into account conformational changes of the pocket during binding, and the potential contribution to binding affinities. This may play a

Table 2 Correlations of docking scores calculated for 32 docked poses of pyrimethamine analogues (docking performed with GOLD) vs. experimental pKi value

Scoring function	Correlation coefficient (R^2)	Correlation Coefficient (R^2): (re-minimized pose)
Molegro		
Protein-ligand interaction	0.68	0.52
MolDockScore	0.61	0.42
Accelrys' discovery suite		
LigScore1_Dreiding	0.69	0.67
LigScore2_Dreiding	0.58	0.72
PLP1	0.65	0.56
PLP2	0.60	0.58
Jain	0.57	0.55
PMF	0.51	0.51
Xscore		
Xscore (avg)	0.50	0.44
Hpscore	0.53	0.53
Hmscore	0.47	0.42
Hsscore	0.35	0.32
GOLD		
GOLDscore	0.62	n/a

significant role in the low correlation coefficients presented in Table 2 [31, 32]. This lack of conformational flexibility may also account for the fact that docking experiments with the poor binders P4, P5 and 1 h all resulted in unrealistic poses.

In an attempt to improve the correlation with experimental pK_i values, Accelrys' Discovery Suite was used to re-minimize the docked poses using the CHARMm force field [44] within the environment of the binding site. These re-minimized poses were then rescored with each scoring function. With the exception of LigScore2, the correlation coefficients for all scoring functions decreased (Table 2).
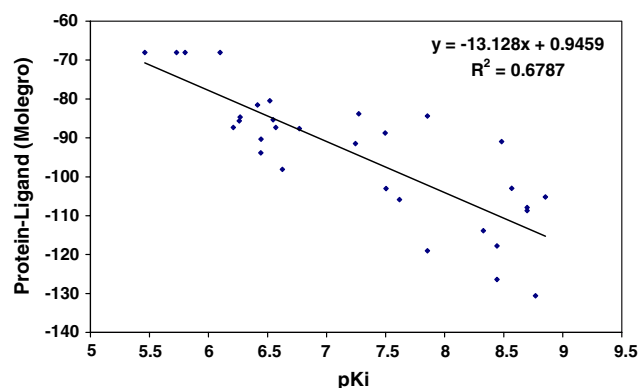
Fig. 5 Correlation of Protein-Ligand Interaction scores (Molegro) calculated for 32 docked poses of pyrimethamine analogues (docking performed with GOLD) vs. experimental pK_i values

As Molegro was already being used for pose selection, and given the marginal difference with LigScore1, the Protein-Ligand Interaction scoring function from Molegro was used for these studies. The correlation of scores to experimental pK_i is presented in Fig. 5.

Discussion

Structural basis for resistance

For the eventual development of novel inhibitors of both wild-type and mutant malarial strains, it is important to develop an understanding of the structural basis of resistance versus activity in the mutant strain. The x-ray crystal structures of WR99210 bound to both wild-type (1J3I.pdb) and the quadruple mutant (1J3k.pdb) DHFR are an excellent starting point.

Two key hydrogen bonding interactions with residues Asp 54 and Ile 14 discussed previously are highlighted in Fig. 4. WR99210 in the quadruple mutant binding site appears to have two H-bonds to Asp 54, whereas the in the wild-type binding site there is only one. In addition, polar interactions with Asn 108 (mutated from Ser 108) and Thr 185 exist in the quadruple mutant site, but not in the wild-type DHFR site. These may help contribute to retention of activity. Most of the other key contacts appear conserved. A similar analysis of predicted protein-ligand interactions was performed with pyrimethamine, which unlike WR99210, lost substantial activity against the mutant DHFR. The Ki_{wt} = 0.6 nM, and Ki_{mutant} = 385 nM [16].

A major factor contributing to the resistance of the quadruple mutant lies in a steric clash between the p-chlorophenyl ring of pyrimethamine and the mutated Asn 108 [10, 25]. This result was reproduced by our docking studies (Fig. 6).

Structure-Activity Relationships

Several trends are obvious from an analysis of the R-groups and pKi_{mutant} values presented in Table 1. First, when R4 is a Cl or another bulky group, the compound tends to be inactive vs. mutant DHFR. R4 corresponds to the para- position on the second aromatic ring. Secondly, when R3 is Cl or another bulky group the compound often retains activity. The R3 position corresponds to the meta-position on the second aromatic ring. Lastly, when R1 is a long chain with multiple oxygens, the compounds retain activity.

An analysis of predicted protein-ligand interactions from the docked poses was performed in order to understand the structural origins of these trends. For purposes of

Fig. 6 Key protein-ligand contacts of bound pyrimethamine to: (**a**) WT *Pf*-DHFR (1J3I.pdb) and (**b**) quadruple mutant *Pf*-DHFR (1J3K.pdb)
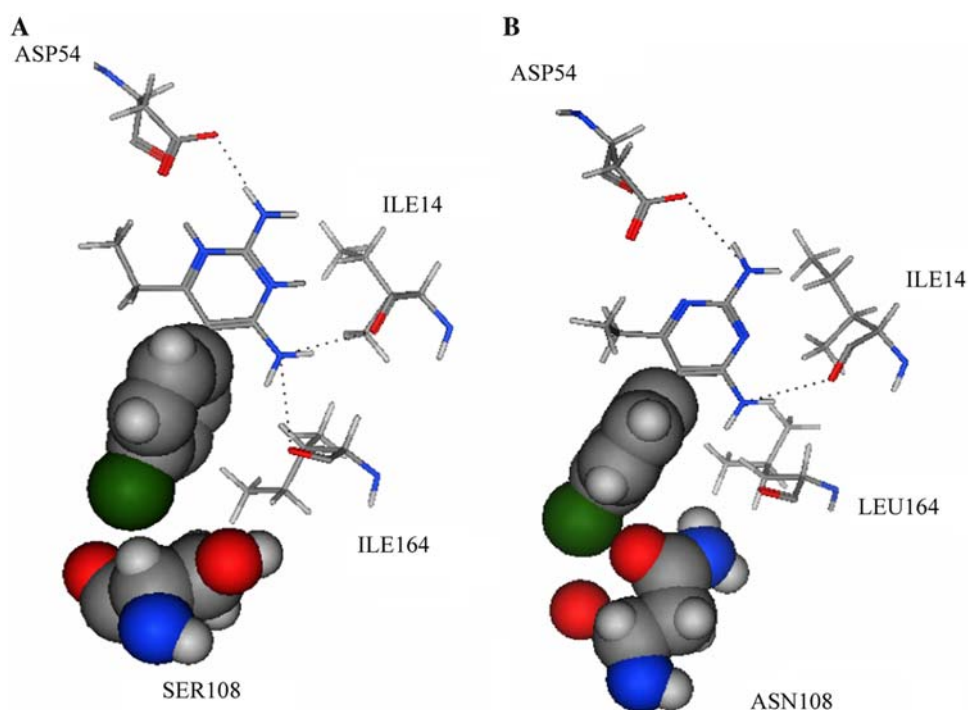
Fig. 7 Predicted protein-ligand contacts of: (**a**) pyrimethamine and (**b**) compound P30 [16]
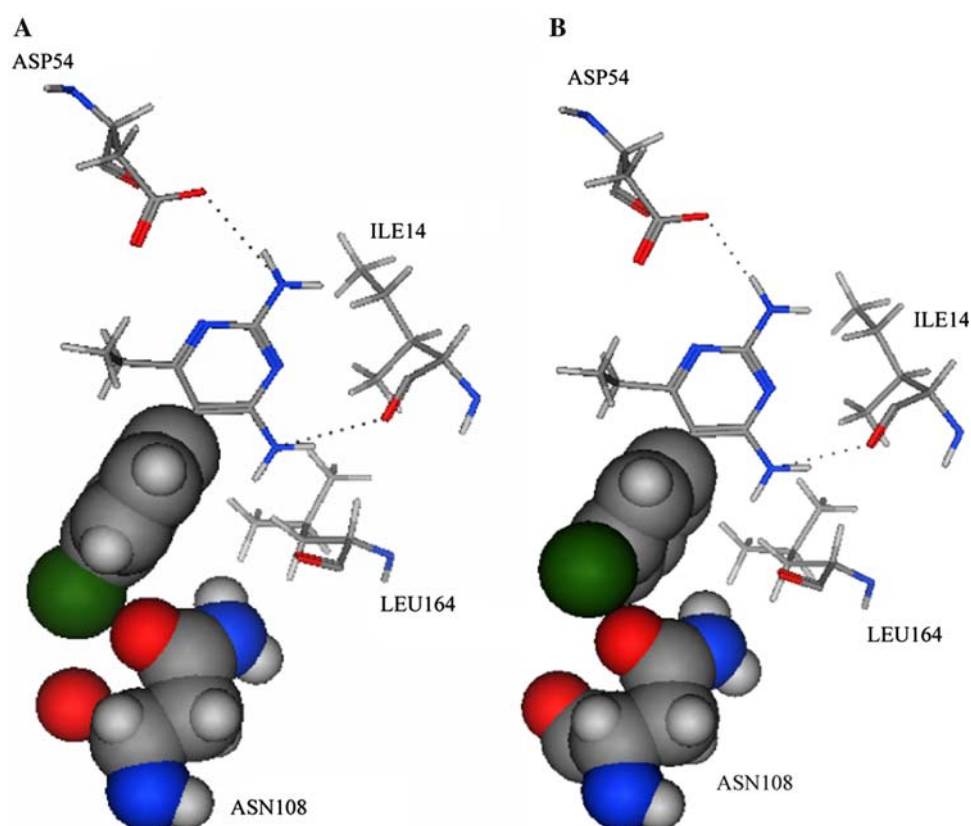

illustration, pyrimethamine (pKi_{mutant} = 6.41) having a Cl at position R4 and a short hydrocarbon chain in position R1 was compared to compound P30 (pKi_{mutant} = 8.48) differing only in the Cl at position R3.

Analysis of key protein-ligand contacts from the poses provides insight into the high potency for compound P30 and lower potency of pyrimethamine. As seen in Fig. 7, both ligands appear to have potential H-bond interactions

Fig. 8 Predicted protein-ligand contacts of: (**a**). compound P16 [16] and (**b**). compound P29.[16]
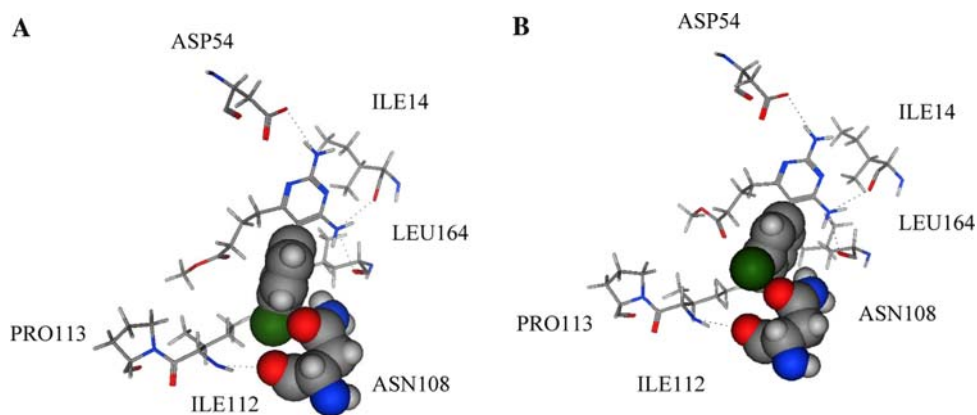
with Asp 54, Ile 14 and Leu 164. However, the para-chlorine from pyrimethamine clashes with Asn 108 and is potentially a source for its poor binding. The meta-chlorine on compound P30 avoids this steric clash.

A second pair of compounds, P16 and P29 were similarly analyzed. Compound P16 (pKi_{mutant} = 6.44) has a Cl at position R4 whereas compound P29 (pKi_{mutant} = 8.57) has a Cl in the R3 position. Both P16 and P29 have the same -$(CH_2)_3COOCH_3$ group in the R1 position.

As seen in Fig. 8, both ligands appear to have potential H-bond interactions with Asp 54, Ile 14 and Leu 164. However, as was the case for pyrimethamine, the less potent compound P16 has chlorine in the para position that appears to clash with Asn 108. The more potent compound P29 on the other hand, has its chlorine in the meta position thus avoiding this unfavorable interaction.

Additional protein-ligand interactions (e.g., van der Waals and/or hydrophobic) are picked up (by both P16 and P29) with Ile 111 and Pro 112. These differences in predicted binding modes, and protein-ligand interactions are consistent with their relative docking scores.

Conclusions

In traditional high-throughput screening (HTS), the greatest source of inefficiency arises from the high percentage of compounds tested that have low probability of ultimate success. Ideally, potent compounds have IC_{50} values in the sub-nanomolar range. Unfortunately, most "reproducible hits" have IC_{50}'s in the low μM to the high nM range and are often non-selective (for the target) thus requiring significant additional medicinal chemistry and biochemistry efforts to optimize.

Because of the expense of traditional HTS screening ($\sim$\$1 per data point) and the high attrition rate of its hits, *in silico* screening is routinely used to generate small focused screening libraries with enriched hit rates. The most effective screens take advantage of available structural data and provide testable SAR hypotheses.

Here we present an application of an *in silico* screening approach using known inhibitors of the quadruple mutant *Pf*-DHFR. This approach generated models that not only provided details of the binding mode and the key molecular interactions but also allowed for prediction of relative inhibition and binding affinities for anti-malarial compounds. This technology can result not only in enriched collections of novel small molecule compounds that bind to protein targets (at least compared to those commercially available), but provides opportunities for medicinal chemists to generate testable SAR hypotheses for lead optimization and development. The approach was first tested on known DHFR inhibitors in order to refine the methodology before application to novel anti-malarial drug discovery, which is the focus of future research.

References

1. National Center for Infectious Diseases, Division of Parasitic Diseases (2007) Internet references. Retrieved from http://www.cdc.gov/malaria/facts.htm 11/4/2006
2. Wells J (2005) Retrieved from http://www.sfgate.com/cgi-bin/article.cgi?file=/c/a/2005/06/05/CMG3NCLBKA1.DTL 4/1/2007
3. WHO Publication (2003) Retrieved from http://www.rbm.who.int/amd2003/amr2003/pdf/ch2.pdf 4/1/2007
4. Hyde JE (2002) Microbes Infect 4:165
5. Yuthavong Y (2002) Microbes Infect 4:175
6. Sibley CH, Ringwald P (2006) Malar J 5:48
7. Ferone R (1977) Bull World Health Organ 55:291
8. Huennekens FM (1994) Adv Enzyme Regul 34:397
9. Rollo IM (1970) CRC Crit Rev Clin Lab Sci 1:565

10. Yuvaniyama J, Chitnumsub P, Kamchonwongpaison S, Vanichtanankul J, Sirawaraporn W, Taylor P, Walkinshaw M, Yuthavong Y (2003) Nat Struct Biol 10:357
11. Sirawaraporn W, Sathikul T, Sirawaraporn R, Yuthavong Y, Santi DV (1997) Proc Natl Acad Sci USA 94:1124
12. Kongsaeree P, Khongsuk P, Leartsakulpanich U, Chitnumsub P, Tarnchombpoo B, Walkinshaw MD, Yuthavong Y (2005) Proc Natl Acad Sci USA 102:13046
13. Mehlin C (2005) Comb Chem High Throughput Screen 8:5
14. Brady RL, Cameron A (2004) Curr Drug Targets 5:137
15. Delfino RT, Santos-Filho OA, Figueroa-Villar JD (2002) Biophys Chem 98:287
16. Kamchonwongpaison S, Quarrell R, Charoensetakul N, Ponsinet R, Vilaivan T, Vanichtanankul J, Tarnchampoo W, Sirawaraporn W, Lowe G, Yuthavong Y (2004) J Med Chem, 47:673
17. Parenti MD, Pacchioni S, Ferrari AM, Rastelli G (2004) J Med Chem 47:4258
18. Agrawal VK, Sohgaura R, Khadikar PV (2002) Bioorg Med Chem 10:2919
19. Mattioni BE, Jurs PC (2003) J Mol Graph Model 21:391
20. Gangjee A, Lee X (2005) J Med Chem 48:1448
21. Sutherland JJ, Weaver DF (2004) J Comput Aided Drug Des 18:309
22. Ganjee A, Lin X (2005) J Med Chem 48:1448
23. Santos-Filho OA, Hopfinger AJ (2001) J Comput Aided Mol Des 15:1
24. Chiu T-L, So S-S (2004) J Chem Inf Comput Sci 44:154
25. Hunt SY, Detering C, Varani G, Jacobus DP, Schiehser GA, Shieh H-M, Nevchas I, Terpinski J, Sibley CH (2005) Mol Biochem Parasitol 144:198
26. Bissantz C, Folkers G, Rognan D (2000) J Med Chem 43:4759
27. Wang R, Lai L, Wang S (2002) J Comput-Aided Mol Des 16:11
28. Wang R, Liu L, Lai L, Tang Y (1998) J Mol Model 4:379
29. Warren GL et al (2006) J Med Chem 49:5912
30. Kitchen DB et al (2004) Nat Rev Drug Discov 3:935
31. Teodoro ML, Kavraki LE (2003) Curr Pharm Des 9:1635
32. Cavasotto CN, Abagyan RA (2004) J Mol Biol 337:209
33. Guex N, Peitsch MC (1997) Electrophoresis 18:2714
34. Molecular Operation Environment. MOE Molecular Operating Environment, Chemical Computing Group, Montreal, Quebec, Canada (2005) Retrieved from http://www.chemcomp.com 4/1/2007
35. Jones G, Willett P, Glen RC, Leach AR, Taylor R (1997) J Mol Biol, 267:727
36. Chemdraw, Cambridgesoft, Inc., Cambridge, MA (2007) Retrieved from http://www.camsoft.com 4/1/2007
37. Halgren TA (1996) J Comp Chem 17:490
38. Thomsen R, Christensen MH (2006) J Med Chem 49:3315
39. Krammer A, Kirchhoff PD, Jiang X, Venkatachalam CM, Waldman M (2005) J Mol Graph Model 23:395
40. Gehlhaar DK, Verkhivker GM, Rejto PA, Sherman CJ, Fogel DB, Fogel LJ, Freer ST (1995) Chem Biol 2:317
41. Gehlhaar DK, Bouzida D, Rejto PA, In: Parrill L, Rami Reddy M (eds), Rational drug design: novel methodology and practical applications, American Chemical Society, Washington, DC (1999), 292
42. Jain AN (1996) J Comput Aided Mol Des 10:427
43. Muegge I, Martin YCA (1999) J Med Chem 42:791
44. Brooks BR, Bruccoleri RE, Olafson BD, States DJ, Swaminathan S, Karplus M (1983) J Comp Chem 4:187